

Chem Soc Rev

Chemical Society Reviews

www.rsc.org/chemsocrev



Themed issue: Nucleation and crystallisation

ISSN 0306-0012



Guest editors: David Amabilino and Xavier Obradors

TUTORIAL REVIEW

Fermín Otálora and JuanMa García-Ruiz

Nucleation and growth of the Naica giant gypsum crystals

Nucleation and growth of the Naica giant gypsum crystals

Cite this: *Chem. Soc. Rev.*, 2014, 43, 2013

Fermin Otálora* and JuanMa García-Ruiz*

Received 5th September 2013

DOI: 10.1039/c3cs60320b

www.rsc.org/csr

The Cave of Giant Crystals in the Naica mine (Mexico) is one of the most amazing displays of mineral beauty ever created in nature. In addition to the colossal crystals of gypsum, which in some cases exceed eleven meters in length and one meter in thickness, the scenery fashioned by the crystalline beams that thrust through the darkness of the cave from floor to ceiling with a luster like moonlight is a unique example of harmony based on crystal symmetry. We review the crystallogensis of this remarkable and challenging phenomenon of mineralization near equilibrium that can be used to teach the basics of nucleation and crystal growth.

Key learning points

1. Crystal nucleation and growth kinetics; applications in decoding the origin of natural mineral systems.
2. The giant gypsum crystals in Naica as a prototype of close to equilibrium crystallization at a very low nucleation rate.
3. The anhydrite–gypsum thermally driven transformation as a self-feeding mechanism providing very low supersaturation solutions with very stable composition.
4. Exploring the different growth mechanisms to understand the growth and morphology of crystals at very low supersaturation.

1 Introduction

The existence of giant crystals hidden beneath the surface of the Earth has long been an appealing idea that has won a place in the collective imagination. The dream started to take shape in the 18th century when the Europe of the Enlightenment was amazed by the crystalline minerals collected worldwide and displayed and classified in the cabinets and Natural History Museums. At the beginning of the 19th century, these mineral collections triggered the foundation of the modern theory of crystals by Rome de L'Isle and René Haüy. It was also at that time when crystals permeated culture and artists like Goethe became fascinated by the geometrical perfection of crystals. However, the idea of a scenario of giant crystals was probably best evoked during the second part of the 19th century by Jules Verne in his very successful book *Voyage au centre de la Terre*,¹ as well as by George Sand in her romantic novel *Voyage dans le cristal*.² Later on, during the 20th century the plausible existence of big crystals was reworked in science-fiction literature, comics and scripts for radio or TV programs. The one that had a worldwide impact on several generations is surely the mythical

hero Superman and the crystals from Krypton, his fictional home planet, and the Memory Crystals from the Fortress of Solitude.³

The closest mineral scenario to the dreams of fictional literature has actually been found beneath the desert in Naica, a mining town in the Mexican state of Chihuahua. They are not the largest crystals found in nature,^{4–6} but they are certainly the largest ones that have grown freely in shape and display themselves as a spectacular cluster of individual crystals of gypsum decorating a large limestone cave. As shown in Fig. 1, the giant crystals of Naica create an unforgettable picture, not only because of the size and shape of the columnar crystals (up to almost 12 meters long) crisscrossing the large cave, but also because of their moonlike brightness that contrasts with the brown (iron coated limestone) walls of the cave.

Nevertheless, behind that beauty lies a formidable challenge for scientific research to explore their formation. When designing crystallization experiments in the lab, we try to find correlations between controlled experimental conditions and the properties (number, size, quality, *etc.*) of the forming crystals. When facing a problem of mineral growth from natural samples, we have only the final output of the “experiment”: the grown crystals, *i.e.* the crystals that once grew in a given geological scenario. Therefore, except for present-day mineral growth processes, we have to decode the information

LEC, IACT (CSIC/UGr), Av. de Las Palmeras 4, Armilla (Granada), Spain.
E-mail: fermin@lec.csic.es, jmgruiz@ugr.es; Fax: +34 958 552 620;
Tel: +34 958 230 000



Fig. 1 The Cave of Giant Crystals in Naica. Picture by Javier Trueba (msf).

contained in these crystals and in their geological environment using the available theories and techniques that allow us to decipher their growth history. But what makes Naica gypsum crystals an even bigger challenge is that we do not have the possibility of mimicking in the lab the conditions in which these crystals could form, namely as the result of a mineralogical process taking place close to equilibrium and with very slow kinetics. These processes are difficult to quantify, but fortunately it is not impossible to do so.

Thus, the problem of the formation of the giant crystals of Naica provides an excellent opportunity for teaching the subtle but important aspects of crystallization theory that must be known to build a rational understanding of the formation of these fabulous crystals. The two-fold aim of this paper is to review the current knowledge on the crystallization of giant crystals of gypsum and to teach how to apply the basic concepts of nucleation and crystal growth theory to decipher a real problem of natural mineral growth.

2 The basic geological and mineralogical information

The giant crystals are made of gypsum, dihydrated calcium sulphate that crystallizes in the monoclinic system showing a layered structure (see, for example, ref. 7). The layers of calcium sulphate and water molecules are stacked along the b -axis, and they are slightly bonded to each other explaining the perfect cleavage of gypsum parallel to the $\{010\}$ faces. Gypsum has several varieties with different shapes and texture arrangements.⁸ A variety named “gypsum alabaster” is made of fine-grained crystals and is used for craftwork. The “satin spar” is a variety made of tiny fibrous crystals that has an attractive silky luster, and the variety of gypsum called “selenite” is characterized by colorless and transparent crystals. This latter variety is the one found mostly in Naica.

Calcium sulphate also crystallizes as two other minerals that are relevant to gypsum crystallization.^{9,10} One of them is anhydrite, the anhydrous calcium sulphate that in contrast to the dihydrate crystallizes in the orthorhombic system. The third form is bassanite, the hemihydrate of calcium sulphate that crystallizes in the hexagonal system. Gypsum is the stable phase forming at room temperature while anhydrite forms at higher temperatures. As we will see below there are discrepancies in the temperature at which gypsum and anhydrite solubilities are equal, *i.e.* the temperature of transition between both phases.

The Naica mining district is located in the south-central area of the State of Chihuahua (Mexico), within the municipality of Saucillo. Its geographical coordinates are North $27^{\circ} 51'20''$; West $105^{\circ} 27'00''$. It is a well known mine that has exploited minerals of zinc, lead and silver since the 19th century. The ore minerals are characteristic of a sulphide-skarn deposit that formed at high temperature in the range between 680°C and 120°C .^{11,12} Actually, gypsum is not among the ores exploited in the mine, although it appears everywhere filling cavities of



Fermín Otálora

Fermín Otálora was awarded a PhD in Earth Sciences from Granada University (Spain) in 1994. After a postdoctoral period at the European Synchrotron Radiation Facility (Grenoble, France), he joined in 1996 the Laboratorio de Estudios Cristalográficos (IACT, CSIC/UGr) in Granada. His research activities at LEC include studies of nucleation and crystal growth kinetics in mineral systems and biomacromolecules, computer

simulation of crystal growth, characterization of crystal quality by X-ray diffraction, in situ optical diagnostics for crystal growth processes, and microgravity crystal growth.



JuanMa García-Ruiz

Juanma García-Ruiz (Sevilla, Spain, 1953) is Research Professor of the Spanish National Research Council (CSIC). His research interest focuses on (a) pattern formation in geological and biomineral structures, with implications from the origin of life to the synthesis of new materials, and (b) the challenges in the crystallization of chemicals, drugs, and macromolecules. He is the founder of the Laboratorio de Estudios Cristalográficos and the

chair of the Spanish Factoría de Cristalización. He also enjoys playing flamenco guitar and writing scientific outreach (<http://garciaruiz.com/JuanMa.html>).

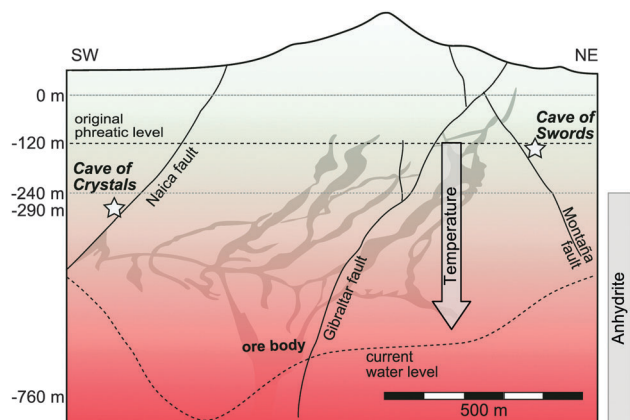


Fig. 2 Vertical cross section of the Naica mine.

different shapes and sizes, always in the form of large selenite crystals of high transparency. Fig. 2 shows a cross section of the mine with the main geologic information relevant for a review of the crystallization of these megacrystals. The mountain is formed of sedimentary rocks, consisting of a sequence of Albian limestones (112.0 ± 1.0 Ma to 99.6 ± 0.9 Ma, million years old) with some clay and salt interbeddings. Mineralization was provoked by an intrusive magma that injected metal rich acidic fluids about 30 to 26 Ma.^{13,14} Note the existence of three main faults, namely, Naica, Gibraltar and Montaña. These faults are very important for fluid circulation within the mountain, and noticeably, most caves with large gypsum crystals are always close to these faults.

There are many caves and cavities filled with gypsum crystals within the mountain of Naica. For the sake of clarity we can differentiate two main caves. One is the “Cave of Swords”, discovered in 1910,^{15,16} which is located near the Montaña fault within the oxidation zone, *i.e.* above the level reached by percolating rainwater, -130 m in the case of Naica district (hereinafter the depths are denoted by the vertical distance to the mine entrance, “level 0”, located at 1385 m above sea level). The walls, ceiling and floor of this cave are completely covered with crystals of tens of centimetres in length, of two different morphologies (habit), as well as some aggregates of large elongated crystals up to 2 meters in size also called “magueys”. The crystals contain lots of fluid and solid inclusions, and in many cases are coated by aragonite and calcite.¹⁷ There are many other caves and cavities below the oxidation zone. Among them, the most studied one, discovered in 2000, is the so-called “Cave of Crystals”, but that should be called the “Cave of Giant Crystals”. Compared to the Cave of Swords, in the Cave of Giant Crystals the number of crystals is much smaller, and the crystals are larger and more transparent and free from solid inclusions. The crystals in this cave also display two different morphologies as in the Cave of Swords, namely the blocky crystals and the columnar crystals of up to eleven meters in size.¹⁸

Relevant information for the understanding of gypsum precipitation in Naica is the presence of anhydrite, the anhydrous phase of calcium sulphate, in the lower levels of the mine.

The anhydrite has two origins, one being formed during the later stages of hydrothermal events (“hypogenic anhydrite”),^{19,20} and the other being sedimentary anhydrite intercalated with limestone in the hundred-meter thick Aurora formation. These anhydrite layers are located at the same levels (from -240 to -590 m) as those of the gypsum caves containing larger crystals, and we will see that they also acted as sources of SO_4^{2-} and Ca^{2+} for the growth of gypsum crystals.

Another important piece of information concerns the underground water of Naica. The upper level of groundwater (the “phreatic level”) is above most of the galleries and pumping of large volumes of water is needed to lower this level and allow mining activities. The Naica area is still under a mild thermal anomaly and water springing in the mine galleries has a temperature ranging from 50 to 60 °C.²¹ There is not yet a map of temperatures within the mountain but there is certainly a thermal gradient (for instance the temperature in the Cave of Swords was measured at 39 °C in the summer of 2012) that must certainly be influenced by the continuous pumping of water that enables mining activities. Actually, the original phreatic level of the mine was located at -120 m. To allow deeper mining, the phreatic level has gradually been lowered by pumping enormous volumes of water, as much as 110 m³ per minute in 2012. It is unknown if the Cave of Swords was dry at the time the miners were mining the level of that cave as it is located very close to the original phreatic level. But certainly, the crystals of the Cave of Giant Crystals were underwater at least up to 1976, soon before the level -290 was drained to allow mining. Currently, the phreatic level is located at -390 while at the center of the depletion cone, the water table is located at about -820.

The concentration of CaSO_4 in the current groundwater in Naica is very close to the solubility of both gypsum and anhydrite. In fact the difference lies within the error of the analytical methods used for measuring the concentration of the ions. Salinity of this water is low, pH is around 7.6, and the Sr concentration is anomalously high.

Since their extraordinary size is the most amazing feature of the crystals of Naica, the first question that comes to mind is “Why are they so big?” However, what puzzles a crystal grower is not only the size but also the low number of crystals within the cave. At first sight the noticeable difference in the number of crystals in the upper Cave of Swords and the deeper Cave of Giant Crystals is striking. In the upper cave the crystals are smaller but more abundant than in the Cave of Crystals, where there are fewer but of much greater size. Actually, the right question to ask is why there are so few crystals in these caves. The answer to this question has to be found in the process leading to the initial formation of crystals, *i.e.* nucleation. In fact, the formation of the large crystals of Naica is rather a problem of nucleation than a problem of crystal growth. Let us see why.

3 Nucleation of gypsum crystals

This section introduces only those nucleation concepts required to understand the origin of the giant crystals in Naica.

A full treatment of nucleation can be found in the excellent textbooks by Kashchiev²² or Kelton and Greer.²³ It must be emphasized that nucleation theory is currently under active discussion owing to a large number of experimental reports on observations of nucleation processes at the nanometre scale (see for example ref. 24 and references therein). These new developments, generally called “non-classical” or “two-step” nucleation, are beyond the scope of this review and are not required to understand the formation of giant gypsum crystals. Quantitative conclusions drawn from Classical Nucleation Theory shall be handled carefully, in particular when nucleation happens at high supersaturation (*i.e.* from small nuclei having an ill-defined surface energy) or when the surface energy, even for large nuclei, is not well known. The giant gypsum crystals nucleated at low supersaturation and there are a number of experimental studies on the kinetics of gypsum nucleation, which makes safe enough the numerical estimation of nucleation kinetics.

The number of crystals produced in a supersaturated system is given by the nucleation rate and the time the system spends in the supersaturated state. According to the classical nucleation theory, the nucleation rate in stationary state J_s is

$$J_s = A \exp \frac{-B\gamma^3}{\Delta\mu^2}$$

where A and B are constants depending on the concentration of ions or molecules and the frequencies of molecular vibration and subcritical aggregation. The specific surface energy (γ) and the supersaturation ($\Delta\mu$) are the central parameters for nucleation kinetics. If a condensed system, in this case a solution, containing M monomers undergoes nucleation, leading to a heterogeneous state containing an n -monomers aggregate of a new phase, and $M-n$ monomers in the old phase, the Gibbs free energy changes from

$$G_1 = M\mu_{\text{old}}$$

to

$$G_2(n) = (M - n)\mu_{\text{old}} + n\mu_{\text{new}} + S(n)\gamma$$

where μ_{old} and μ_{new} are respectively the chemical potential of the old and new phases and $S(n)\gamma$ is the excess energy associated with the creation of the interface existing between them. This surface energy is expressed as the product of the surface area $S(n)$ and the specific surface energy γ . γ is inherent to the distribution of molecules and bonds in the crystal surface, while $S(n)$ depends not only on the size but also on the shape of the nucleus, which can be significantly different from that of the final crystal and, therefore, influence nucleation kinetics. The work for aggregate formation is therefore

$$W(n) \equiv G_2(n) - G_1 = -n\Delta\mu + S(n)\gamma \quad (1)$$

where the supersaturation $\Delta\mu = \mu_{\text{old}} - \mu_{\text{new}}$ is the thermodynamic driving force for the phase transition. When $\Delta\mu > 0$ the solution is said to be supersaturated and aggregates of the new phase can form spontaneously; otherwise the solution is said to be undersaturated. Eqn (1) shows the fundamental concepts in

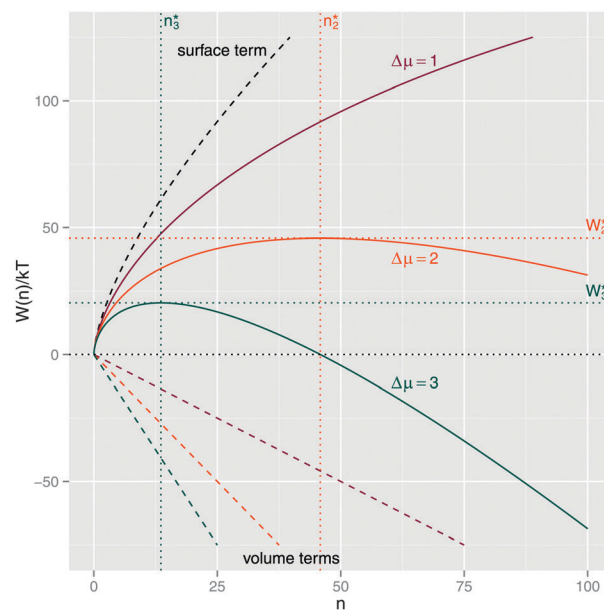


Fig. 3 Plot of $W(n)$ (solid lines) for gypsum nucleation. Curves are shown for $\Delta\mu/kT = 1$ (purple), 2 (orange) and 3 (blue). Volume (coloured dashed) and surface (black dashed) terms are separately represented. The critical size n^* and the amplitude of the energy barrier for nucleation W^* for the cases $\Delta\mu/kT = 2$ and $\Delta\mu/kT = 3$ are indicated by dotted lines.

nucleation thermodynamics: the work required to form an aggregate of the new phase depends on the size n of the aggregate and contains two terms, the first one ($-n\Delta\mu$) related to the change in volume energy, negative and proportional to the first power of n , and the second ($+S(n)\gamma$) related to the change in surface energy, positive and proportional to $n^{2/3}$ (since $S(n) \approx n^{2/3}$). Fig. 3 shows the resultant functional dependency of $W(n)$ with a maximum at a critical cluster size (n^*) having a critical energy $W^* \equiv W(n^*)$, both dependent on the supersaturation and the specific surface energy. Clusters smaller than this critical size are known as “precritical nuclei” and those larger than this value are “supercritical nuclei” that tend to grow spontaneously because this growth decreases their free energy.

The specific surface energy γ is an intrinsic property of the material that can be measured by nucleation experiments detecting the induction time for nucleation

$$t_{\text{ind}} = \frac{1}{J_s V}$$

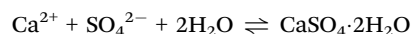
where V is the solution volume. A plot of $\log(t_{\text{ind}})$ versus $1/(\Delta\mu/kT)^2$ produces a straight line with slope $B\gamma^3$. In the case of gypsum, and other compounds, this plot typically shows two linear regions (see, for example, ref. 25), with a larger slope for high supersaturation values and a smaller slope at low supersaturation. This behaviour is due to a change in the nucleation mechanism, leading to an apparent decrease of γ at low supersaturation, where nucleation is heterogeneous, *i.e.* it happens on pre-existent surfaces or colloidal particles, so the surface area $S(n)$ of the nuclei is smaller for the same cluster volume. This kind of experiment for gypsum²⁵ yields a value $\gamma = 37 \text{ mJ m}^{-2}$,

which gets reduced by a factor of 6.9 in the region of heterogeneous nucleation. This value, which we will use in our calculations, corresponds to the unknown substrates on which gypsum nucleated during the experiment of Lancia *et al.* As the reduction in surface energy depends on the contact angle between gypsum and the substrate, it is different for different surfaces or particles, so this value is just a reasonable approximation based on previous experiments.

$\Delta\mu$ is proportional to the logarithm of the ratio between the actual and the equilibrium value of the thermodynamic variable h driving nucleation

$$\Delta\mu = kT \log \frac{h}{h_{\text{eq}}}$$

where the subscript “eq” indicates “at equilibrium” and the variable h can be the pressure (in gas condensation), temperature (in solidification from melt), solute activity (in nucleation from mono-component solutions), or ionic activity product (in nucleation from multi-component ionic solutions). The last case is the one relevant for the crystallization of gypsum by the reaction



that describes, in terms of mass-action law, the precipitation (left to right) or dissolution (right to left) of gypsum from Ca^{2+} and SO_4^{2-} ions in solution. This equilibrium is characterized by a thermodynamic equilibrium constant K_{sp} called “solubility product”

$$K_{\text{sp}} = \frac{a_{\text{Ca}^{2+}} a_{\text{SO}_4^{2-}} a_{\text{H}_2\text{O}}^2}{a_{\text{CaSO}_4 \cdot 2\text{H}_2\text{O}}} \Big|_{\text{eq}} \quad (2)$$

where a_i means “activity of i ”. Since the activity of the solid phase is assumed to be constant and equal to 1, the equilibrium constant simplifies to the “Ion Activity Product” Π at equilibrium

$$\Pi = a_{\text{Ca}^{2+}} a_{\text{SO}_4^{2-}} a_{\text{H}_2\text{O}}^2 \quad (3)$$

$$K_{\text{sp}} = \Pi_{\text{eq}}, \quad (4)$$

so that

$$\Delta\mu = kT \log \frac{\Pi}{K_{\text{sp}}} \quad (5)$$

In crystal growth literature, the driving force for nucleation and growth is often expressed in terms of “relative supersaturation”,

$$\sigma = \frac{(C - C_{\text{eq}})}{C_{\text{eq}}} = \frac{C}{C_{\text{eq}}} - 1$$

as a first order approximation of $\Delta\mu/kT$ for small supersaturation values since $\log(x) = (x - 1) - (x - 1)^2/2 + (x - 1)^3/3 - \dots$. In crystal growth kinetics, the most commonly used quantity is the “absolute supersaturation” $\sigma_a = C_{\text{eq}}\sigma = (C - C_{\text{eq}})$. Finally, in geological literature, the same concept is expressed by the “Saturation Index” $\text{SI} = \log_{10}(\Pi/K_{\text{sp}})$.²⁶

The previous expression for $\Delta\mu$ in the crystallization of gypsum immediately suggests the two basic ways of getting a solution supersaturated and, therefore, driving nucleation: (a) changing Π through changes in the activity of reactants, either those involved in the reaction or others modifying the ionic strength or solvent interactions; and (b) changing K_{sp} through changes either in temperature or in the concentration of chemicals that modify the inter-monomer interactions. As in any other chemical equilibria, the solubility product is temperature-dependent. The van't Hoff equation in chemical thermodynamics relates the change in K_{sp} to the change in temperature, given the standard enthalpy change ΔH_0 for the process, but typically the behaviour is non-linear and a better approximation for $K_{\text{sp}}(T)$ is obtained using analytical expressions derived by fitting experimental data.²⁷

Owing to the dependency on $\exp(-1/(\Delta\mu)^2)$, the nucleation rate $J_s(\Delta\mu)$ is a very steep function (see Fig. 6 later). For very small supersaturation values, nucleation is extremely unlikely, and for larger values, it increases very quickly. A small or medium nucleation rate is possible only in a very narrow region around the threshold triggering massive precipitation. This means that nucleation kinetics is extremely sensitive, so even small changes in supersaturation can lead to many orders of magnitude changes in the number of crystals produced. Therefore the answer to the question about the giant Naica crystals, “Why there are so few?”, is “Because they nucleated at very low supersaturation”. This is the only way to keep the number of crystals low enough so that each of them may grow later to a very large size. Even more, the supersaturation must be kept low for the whole crystal growth history, at least low enough to avoid triggering massive nucleation. Any geochemical system that we could imagine to explain the formation of giant crystals must exclude any high amplitude fluctuation of the supersaturation value.

The above discussion explains the number of crystals, What about the size? Each of the large beams in the Cave of Crystals weighs more than 5 tons (that is about 32 000 moles). Just one of these crystals is enough to saturate with respect to gypsum the water contained in the whole volume of the cave (3000 m³) assuming that it was a closed system. Therefore, the growth of these huge crystals is only possible if Naica is an open system receiving a small and very steady supply of Ca^{2+} and SO_4^{2-} ions during a very long period of time, while keeping supersaturation low. What mechanism, consistent with the geological setting of Naica, is able to produce a large yet slow and steady supply of calcium sulphate over a long period of time?

4 A plausible genetic mechanism

As proposed by García-Ruiz *et al.*,²¹ these giant crystals are the result of a self-feeding mechanism based on a solution-mediated anhydrite-gypsum phase transition occurring in a slow and smooth cooling scenario. Let us explain it:

As discussed in Section 2, calcium sulphate may precipitate in three different forms, each of them stable in a different

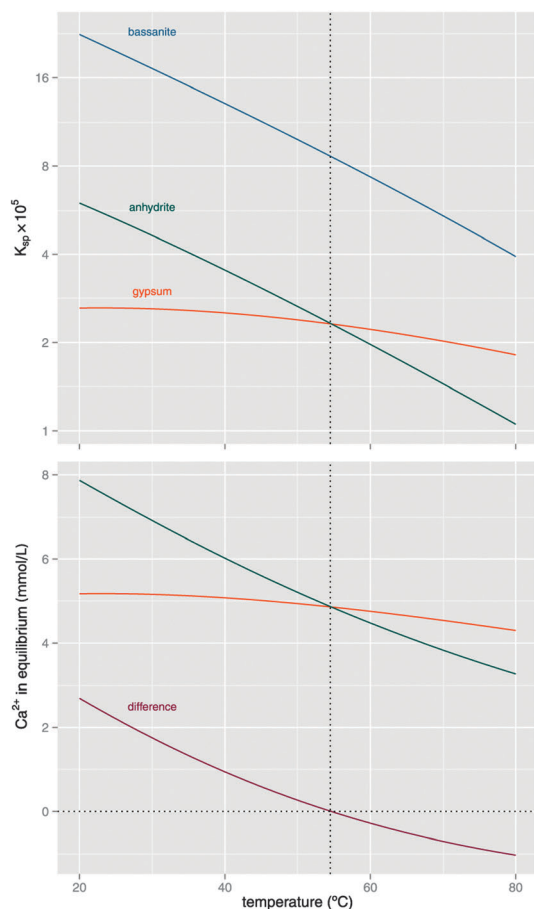


Fig. 4 Top: solubility product (K_{sp}) as a function of temperature for gypsum, bassanite and anhydrite. The dotted vertical line indicates the transition temperature between the fields of stability of gypsum at low temperature and anhydrite at high temperature. Bottom: Ca^{2+} in equilibrium (separately) with anhydrite and gypsum as a function of temperature; the difference in concentration is the net source of ions “pumped” by solution cooling. All data computed from the phase databases phreeqc.dat (for gypsum and anhydrite) and llnl.dat (for bassanite) of the geochemical software Phreeqc (version 3.0.6).²⁷

temperature range, as shown in Fig. 4 (top). The hemihydrate is the most soluble phase over the whole temperature range plotted, while the dihydrate is the most stable (less soluble) phase at low temperature (below 54.5 °C) and the anhydrous calcium sulphate is the stable phase above this temperature. The existence of a crossover between the solubility of anhydrite and gypsum provides the “ion pump” required for a steady and continuous supply of growth units. Fig. 4 (bottom) shows the solubility of gypsum and anhydrite plotted against temperature along with the difference in solubility that is the maximum amount of Ca^{2+} and SO_4^{2-} ions transferred from anhydrite to gypsum (or the other way around if negative) as a function of temperature. This amount is small enough to ensure a slow and steady supply ($\pm 10^{-3}$ moles per litre in the 40–80 °C range).

What we propose is that this “ion pump”—based on the anhydrite–gypsum transformation—in operation in the Naica range is driven by the slow cooling of the mountain after the magmatic intrusion, leading to the close-to-equilibrium anhydrite

dissolution and gypsum growth at progressively lower levels within the phreatic layer. This mechanism requires two main conditions to operate:

- There must be enough anhydrite in the area.
- The temperature at which the crystals grow must be close to (but lower than) the transition temperature (54.5 °C).

Both conditions are met in Naica, as explained in Section 2. Information on the temperature of both current groundwater and the solution in equilibrium with the crystals during their growth (from fluid inclusions trapped in the crystals) shows that this is the case:^{21,28} Current groundwater has a mean temperature of $T = 53.2 \pm 0.8$ °C while fluid inclusions indicate $T = 52.5 \pm 4.6$ °C during crystal growth, corresponding to a very low undersaturation for anhydrite ($\Delta\mu/kT = -0.04$).

A word of caution is in order here. The anhydrite–gypsum transition temperature has been an active field of research (see ref. 29–32 and references therein), the exact value being very elusive and variable in different works due to differences in the experimental setup and in the composition of the solutions studied. Since the thermodynamic data available in databases come from fits to experimental data, this uncertainty pervades theoretical studies and works making use of this information, as in the case of this paper. This situation can be illustrated, for example, by comparing the calculations in this paper with our previous results²¹ in which the transition temperature was computed to be 58 °C. The previous work was done using version 2 of the Phreeqc software,²⁷ updated to version 3 at the time of the present work. The thermodynamic data for anhydrite have been updated in the database used by the software for the latest version, leading to a different $K_{sp}(T)$ curve for this phase and, consequently, to a different transition temperature. Lacking a strong rationale to prefer one set of thermodynamic data over the other, we decided to make the calculations with the new one and to mention the fact as a warning about these uncertainties of 3.5 °C (possibly even larger using other databases or software packages) when dealing with published data in this context.

A number of additional pieces of evidence support this self-feeding mechanism for the nucleation and growth of the giant gypsum crystals:²¹ fluid inclusions in the gypsum crystals also show that they grew from low salinity water, different from those giving rise to anhydrite. The isotopic composition of these crystals ($\delta^{34}\text{S}$ versus $\delta^{18}\text{O}$) shows that the crystals grew from a mix of (a) water enriched in SO_4^{2-} from the dissolution of anhydrite at different locations of the mine, (b) water from the ore deposit area and (c) water from the upper levels. Indirect evidence for the origin of the solution from which gypsum crystals grew are the absence of minerals like alunite or kaolinite, typical of sulphuric speleogenesis mineralizations, and the presence of celestite coating the walls of the Cave of Crystals. Since the structure of anhydrite can hold more strontium as impurity than the structure of gypsum, precipitation of celestite is consistent with the solution-mediated transformation of anhydrite into gypsum.

Fig. 5 compares the supersaturation with respect to gypsum of the current groundwater (dots) and the supersaturation

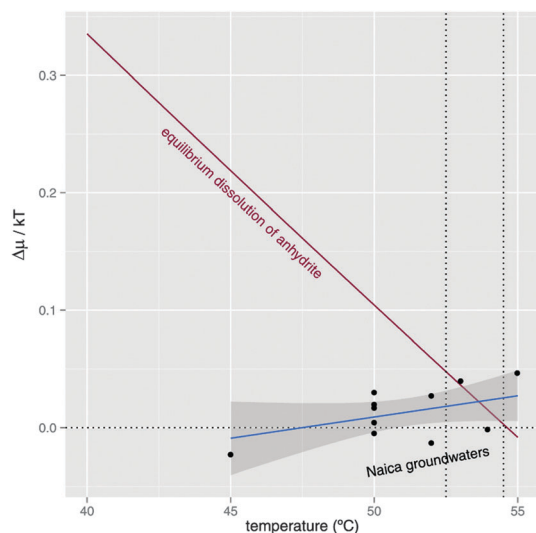


Fig. 5 Supersaturation with respect to gypsum of the Naica groundwater (dots, data from ref. 33). The blue line is a linear regression of the same data, and the dark gray bar indicates the 95% confidence region of this regression. The solid line shows the supersaturation values for solutions obtained by the dissolution of anhydrite at each temperature. The vertical dotted lines indicate the average temperature during the growth of the giant crystals (52.5 °C) from fluid inclusions²¹ and the transition temperature (54.5 °C).

calculated for solutions obtained by the equilibrium dissolution of anhydrite, *i.e.* the supersaturation value predicted by the self-feeding mechanism (solid purple line). The range of temperatures where crystal growth occurs is indicated by the two vertical dotted lines at $T = 52.5$ °C (the crystal growth temperature from fluid inclusion measurements) and $T = 54.5$ °C (the transition temperature). In this temperature range, the supersaturation values of the Naica water are very small and equal to those predicted by the model. This supports the genetic mechanism proposed. For lower temperatures the measured supersaturation diverges from the values expected for water in equilibrium with anhydrite, approaching equilibrium ($\Delta\mu/kT = 0$) as temperature decreases. This is due to Ca^{2+} and SO_4^{2-} consumption due to gypsum crystallization. The distance between both curves is larger for lower temperatures, as expected, because nucleation and growth of gypsum crystals are faster at lower temperatures (higher supersaturation).

Fig. 6 shows the nucleation rate (top) and the induction time (bottom) as a function of temperature computed from solutions obtained by the dissolution of anhydrite. In the range of temperatures shown in Fig. 6 (bottom), the solubility of gypsum is lower than the solubility of anhydrite (except at the extreme right, where both solubility curves cross). Consequently, in this region of the phase diagram, only solution or solution + gypsum may exist in equilibrium, the thermodynamic limit for this coexistence being the gypsum solubility curve (solid orange). The energy barrier for nucleation decreases for conditions further from the solubility curve and at a given distance it is low enough to allow almost instantaneous nucleation events. This limit, along with the equilibrium curve, defines a metastable region where gypsum crystals may appear with different

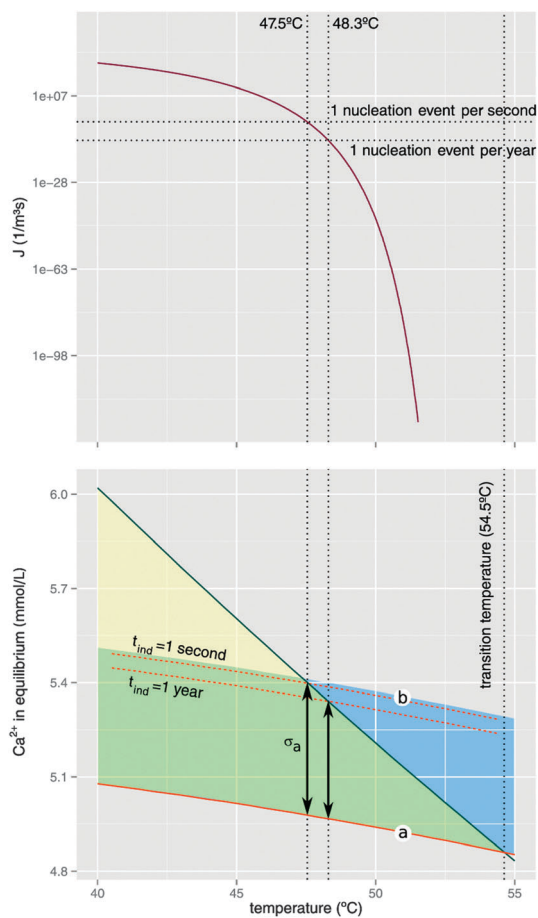


Fig. 6 Nucleation rate (top) for gypsum nucleated from solutions produced by equilibrium dissolution of anhydrite as a function of temperature. The plot at the bottom shows the anhydrite and gypsum solubility and the absolute supersaturation σ (*i.e.* difference in solubility) at two different temperatures. The blue region is the metastable zone for gypsum and the green triangle indicates the range of conditions where the self-feeding mechanism operates.

probabilities (*i.e.* after different average induction times). This region is marked by the blue and green shades and is independent of the processes controlling temperature or solution composition. Fig. 6 also shows the region where the proposed self-feeding mechanism operates. Since this mechanism involved the dissolution of anhydrite and the subsequent growth of gypsum, this region, shaded yellow and green, is obviously the triangle between both solubility curves. The intersection between this two regions (the green area) is, therefore, the region where gypsum crystals can nucleate and grow by the proposed self-feeding mechanism. The yellow region corresponds to conditions leading to micro-crystalline or amorphous precipitates of gypsum while the blue region cannot be reached by close to equilibrium dissolution of anhydrite. The vertical dotted lines indicate the transition temperature and the temperature during the growth of the giant crystals. Nucleation kinetics have been computed assuming heterogeneous nucleation since homogeneous nucleation is impossible from solutions at these extremely low supersaturation values. The two

horizontal dotted lines in the plot indicate $t_{\text{ind}} = 1$ second and 1 year. One nucleation event per second would pack the Cave of Crystals with millions of small crystals while one nucleation event per year would produce a number of crystals compatible with the actual contents of the Cave of Crystals. Nucleation of the giant crystals most likely happened from water at around 48 °C, close to the intersection of the $t_{\text{ind}} = 1$ year and the anhydrite solubility curve.

Finally, the two vertical double arrows joining this “fast kinetics”/“slow kinetics” curves with the equilibrium curve indicate the small change in supersaturation (arrow length difference) and temperature (horizontal distance between arrows) required for these two different regimes of nucleation to happen.

What are the sources of uncertainty in this calculation? There are three main sources: first, the differences between thermodynamic data from different works; the second, the value for the specific surface energy, very important because nucleation rate is proportional to the third power of this energy; and third, the variations in temperature during the growth of the crystals. There are two sources of temperature variations: those induced by the water pumping for mining activities, and those due to the variations of atmospheric temperature during the period in which crystals grew.³⁴ Therefore for a better estimate of the temperature at which crystals nucleate, in the future we need (a) more reliable thermodynamic data on the solubility of gypsum and anhydrite; (b) experimental studies on the heterogeneous nucleation of gypsum on rock forming minerals in Naica; (c) a 3D map of temperatures in the Naica mine that will enable an understanding of the water flow in Naica mines; and (d) the measurement of growth temperature from fluid inclusions in Naica at different points of the crystal along the growth history. This will be a test of the influence of atmospheric variations of temperature on crystals. This influence is evident for the crystals in the Cave of Swords in the upper part of the mine (−120 m) but must be checked in deeper caves.

In any case, we can be sure that temperatures have never been lower than 47 °C, because this would result in induction times of one minute and a nucleation rate of around 3 crystals per second and cubic meter that would fill the cave with millions of small crystals. The next question is: why is the number of crystals in the Cave of Swords much larger than the number of crystals in the Cave of Crystals? This is because according to nucleation theory, what really matters in addition to the change in temperature ΔT (or supersaturation) is the cooling rate.^{35,36} As shown in Fig. 6, the nucleation rate J_s is very low at low supersaturation values and then increases quickly. The plot at the top shows J_s as a function of temperature. The dotted lines indicate two reference rates, one nucleation event per year and one nucleation event per second respectively in the Cave of Crystals. Above approximately 48.3 °C nucleation rates fall quickly to extremely small values, so nucleation is very unlikely to happen. Below 47.5 °C the nucleation rate is too high and a huge number of small crystals would appear. The metastable zone in the solubility plot is

bounded by two curves of different nature. The $\Delta\mu/kT = 0$ boundary is the solubility curve, defined as the *loci* of solutions at equilibrium concentration. The location of this curve is fixed and it is thermodynamic in nature. A solution located on this curve (for example the point labelled “a” in the plot) will be stable forever. The probability of a nucleation event occurring is 0 and the induction time for nucleation is infinite. The upper limit of the metastable zone is named the “metastable limit” or “supersolubility curve” and, unlike the solubility curve, is kinetic in nature and defined as the *loci* of solutions having a probability close to 1 for a nucleation event to occur (for example the point labelled “b” in the plot), so that the induction time for nucleation can be considered 0. Any solution between these limits will nucleate spontaneously given enough time, the induction time being an inverse function of supersaturation. For instance, the two curves (dashed orange lines) in the plot indicate all the points for which the induction time is 1 second and 1 year respectively. If nucleation happens in unsteady conditions, in the case of gypsum this means at variable temperature, the induction time, nucleation rate and probability of nucleation will be variable as well, and nucleation will happen when the residence time at a given temperature (the time spent at that temperature) gets larger than the corresponding induction time. Upon cooling of the solution, the residence time at each temperature will be shorter for higher cooling rates. This means that nucleation will happen at lower temperatures (*i.e.* higher supersaturation and nucleation rate) for faster cooling than for slow cooling rates. In unsteady conditions, therefore, the nucleation rate will depend not only on supersaturation but also on the supersaturation rate, *i.e.* for the case of Naica, on the cooling rate.

Before finishing this section on nucleation, let us ask a simple question: How old are the crystals? The reader may now realize that this question does not have a single, precise answer. The Naica crystallization system was continuously close to equilibrium due to the self-feeding mechanism that dissolves calcium sulphate from anhydrite as soon as gypsum crystallizes. Therefore the system was always moving towards the supersaturated region, with nucleation events taking place continuously at a frequency that depended on the residence time at a given temperature. As a consequence, we can expect that giant crystals nucleated at different times, even long after other crystals were already growing. The relatively large spread in crystal size in the Cave of Crystals supports these heuristics.

Now we move to other exciting questions: What was the growth mechanism of the crystals? At what rate did the crystals grow? Why are there crystals displaying two totally different morphologies? To answer these questions we need some information about the growth mechanism of crystals.

5 Crystal growth

Crystals may grow by three different mechanisms. To introduce them, it is helpful to use a simple model, the Kossel crystal (Fig. 7), in which cubic-shaped monomers having a “bond”

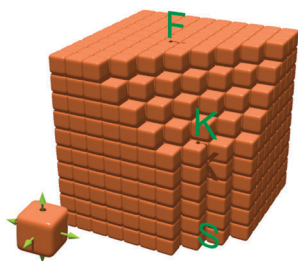


Fig. 7 The toy Kossel model for crystal growth. The crystal is composed of cubic units with six “bonds” in the directions perpendicular to the faces (left bottom). Examples of F, S and K faces are illustrated.

along each of the 6 faces get incorporated into a simple cubic crystal. The faces at the surface of the crystal can have different atomic-level structures depending on their orientation. Three types of faces can be distinguished as a function of the number of bond directions parallel to them; they are labelled in Fig. 7 as F faces (2 or more bonds), S faces (1 bond) and K faces (no bonds).

The “K” in K faces comes from “kink”, which is the name of the surface position where the probability of attaching a monomer and that of detaching a monomer are equal at equilibrium or, what is equivalent, surface energy does not change upon attaching a monomer at this position. When a monomer is attached in a kink position in the K face in Fig. 7, three bonds at the surface get saturated and three new bonds are created, so there is no net change in surface energy. When a face entirely composed of kink positions is in contact with a supersaturated solution, the amount of monomers reaching the surface is proportional to the concentration of monomers in the solution C , while the amount of monomers leaving the surface to the solution is proportional to the equilibrium concentration C_{eq} , so the net growth rate is

$$R = \beta v_0 C_{\text{eq}} S = \beta v_0 (C - C_{\text{eq}}) \quad (6)$$

where $S = \frac{C - C_{\text{eq}}}{C_{\text{eq}}}$ is the relative supersaturation at the surface of the growing crystal (C and C_{eq} being the actual and equilibrium concentration), v_0 is the monomer volume and β is the kinetic coefficient of crystallization

$$\beta = \frac{a\nu(a/\lambda_0)^2}{v_0 C_{\text{eq}}} \exp\left(-\frac{E + \Delta H}{kT}\right)$$

with $a = v_0^{1/3}$ being the linear size of the monomers, ν the molecular vibration frequency in the direction perpendicular to the surface, λ_0 the mean distance between kinks, ΔH the heat of crystallization and E the energy barrier for monomer incorporation into the surface. The term a/λ_0 , equal to 1 in perfect K faces and smaller in imperfect K, S and F faces, makes eqn (6) applicable to all types of faces. Consequently, eqn (6) with $\lambda_0 = a$ is the maximum possible growth rate of a crystal at a given supersaturation. This mechanism of crystallization, called “Normal Growth”, is quite uncommon in solution crystal growth and only occurs at high supersaturation because at low

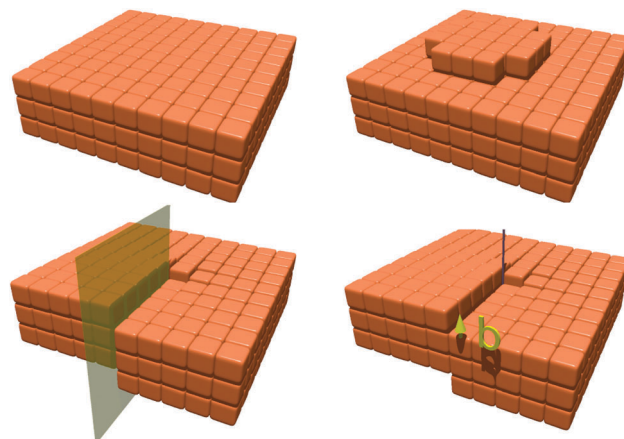


Fig. 8 Top: two-dimensional nucleation. For a perfectly flat face to continue growing, a mono-molecular layer must be started by nucleation of a patch of critical size. From this point on, the face can grow by incorporation of monomers in the kinks and generation of new kinks in the step. Bottom: geometry of the repeatable step produced by screw dislocations.

supersaturation values the density of kinks tends to be minimized.

At lower supersaturation values, the availability of kink positions starts to be a rate limiting process. The extreme case is the growth of perfect F faces (F stands for “flat”). In a perfect F face, there are no kink positions at all (Fig. 8, top left), and to generate kinks a new layer must be started (Fig. 8, top right). Nucleation of a new layer produces kinks at the boundary of the new layer. This boundary is called the “Step”. The mechanism by which a crystal grows by repeated nucleation of two-dimensional layers that then grow by accretion of growth units into the step is called “Two-Dimensional Nucleation Growth”, and the growth rate is limited by the two-dimensional nucleation kinetics. Two-dimensional nucleation is conceptually equivalent to three-dimensional nucleation and physically very similar by just changing volume to surface and surface to length in the derivation of equations. Two different regimes are commonly distinguished within two-dimensional nucleation growth: “Mononuclear Two-Dimensional Nucleation” when the induction time for two-dimensional nucleation is longer than the time required for the new layer to grow until it completely covers the crystal face—this happens at very low supersaturation—and “Polynuclear Two-Dimensional Nucleation” when 2D nucleation and step advancement are simultaneous. This is typical of medium and high supersaturation. Kinetics of the mononuclear mechanism are completely controlled by nucleation because further growth is not possible after the last layer is complete and no more steps exist on the surface. The growth rate of the face is therefore simply

$$R = JL^2a$$

where J is the two-dimensional nucleation rate and L is the linear size of the face. In the polynuclear mechanism, two-dimensional nuclei appear at different points on the surface

and start growing until they meet other partial layers and both steps merge. Growth kinetics are consequently more complex,

$$R = \pi\lambda^2 J a$$

where $\lambda \simeq (v/J\pi)^{1/3}$ is the average radius of the partial layers when they meet and $v = \beta_{\text{st}}v_0(C - C_{\text{eq}})$ is the mean velocity of advancement of the step. The kinetic coefficient in this case is named β_{st} to distinguish it from the normal growth kinetic coefficient β .

Two-dimensional nucleation growth is the most common growth mechanism in solution. As supersaturation increases, λ decreases and the number of partial layers increases; consequently the length of step in the surface and the kink density increase. At a given supersaturation, the kink density is so high that two-dimensional nucleation growth becomes indistinguishable from normal growth. This transition is called ‘‘Kinetic roughening’’ and is the limit between 2D nucleation and normal growth. At the other end, at very low supersaturation values the induction time for two-dimensional nucleation increases as the supersaturation decreases and, for sufficiently small supersaturations, the crystal stops growing because, although the solution is supersaturated, supersaturation is not large enough for two-dimensional nucleation.

At very low supersaturations, crystal growth can be explained by a third mechanism: For a crystal face to grow at very low supersaturation, a source of steps independent of two-dimensional nucleation must exist. Screw dislocations provide this source of steps (Fig. 8, bottom). Screw dislocations are a type of crystal lattice defect formed by displacing, along a half-plane, part of the lattice by a vector \vec{b} (called ‘‘Burgers vector’’) parallel to the edge of the displacement and having a magnitude that is an integer multiple of the lattice spacing of the face. This displacement, produced by mechanical deformations or nucleated during crystal growth, generates a step that can grow at very low supersaturation. During growth, the step goes around the dislocation axis (the vertical line in Fig. 8 bottom) because the step advance rate is slower close to the axis. The layer then grows as a helicoidal staircase. Eventually, the step has rotated a full turn and the situation is now the same as at the beginning, only one layer upwards, so the step generated by a screw dislocation is an infinitely repeatable step, which guarantees the continuous growth even at very low supersaturation. This growth mechanism is called ‘‘Dislocation Growth’’ or ‘‘Spiral Growth’’. Two-dimensional nucleation growth and spiral growth mechanisms are collectively called ‘‘Layer Growth’’. The rate at which the crystals grow by spiral growth is

$$R = \frac{a}{\lambda} v_{\rho}$$

where $\lambda = 2\pi r_c$ is the mean distance between neighbouring turns of the spiral with $r_c = v_0\sigma/\Delta\mu$ the maximum curvature of the step and $v_{\rho} = v(1 - r_c/\rho)$ is the curvature (ρ) dependent step velocity.

Fig. 9 summarizes the different growth mechanisms in terms of the growth rate and supersaturation at which they operate. At low supersaturation, growth proceeds by spiral

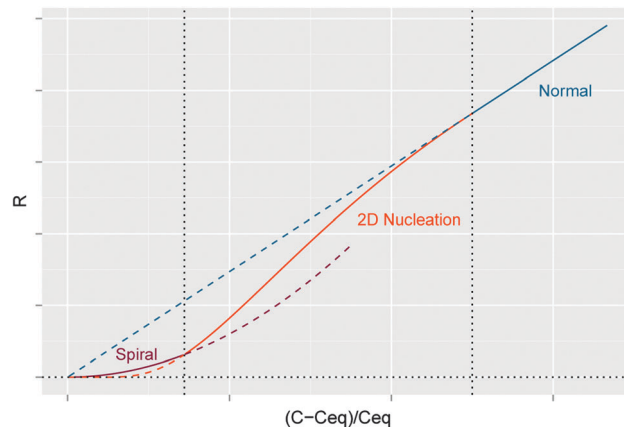


Fig. 9 Sketch of the three crystal growth mechanisms, the supersaturation ranges where they are dominant and the dependence of the functional form on supersaturation.

growth, if screw dislocations exist in the crystal, at a rate approximately proportional to S^2 . In the mid-range of supersaturation values, 2D nucleation is the dominant mechanism and the growth rate changes from $\sim \exp(-K/S)$ at low supersaturation and $\sim S$ at high supersaturation, where the growth rate tends towards the maximum rate of normal growth, linear with S .

5.1 Growth rate

Obviously the Naica giant crystals must have grown at very low supersaturation and therefore should have done so by the spiral growth mechanism. What was their growth rate? The obvious way to answer this question experimentally is to let a gypsum seed to grow in contact with groundwater from Naica. The crystal will grow very slowly for a very long time (1 year or more),³⁷ because the supersaturation of current Naica water is below the experimental error of current analytical techniques for measuring concentration,³³ so significant shifts in supersaturation can be expected when these close-to-equilibrium solutions evaporate even at a very small rate. The alternative is to increase the sensitivity of observation techniques so that much shorter experiments can be implemented to get information in hours on crystal growth processes at very low supersaturation. Understanding the growth of Naica giant crystals has pushed the limits of current technology to measure ultra-slow crystal growth rates using optical diagnostics.³⁸

Studies on gypsum crystal growth kinetics at low and very low supersaturation have concentrated on the $\{010\}$ crystal face because this is the only one growing in these conditions in the 001 zone. $\{1k0\}$ faces develop by advancement of the $\{010\}$ edge and the $\{011\}$ and $\{\bar{1}11\}$ faces have a much lower growth rate.

The growth of gypsum crystals at low supersaturation proceeds mainly by two-dimensional nucleation on $\{010\}$ faces, and the growth rate changes with supersaturation and temperature.³⁹ These studies have shown the nucleation of two-dimensional nuclei, the presence of frequent macrosteps (several stacked steps advancing as a single one with a height that is a multiple of the step height) and the existence of spiral

hillocks although they are relatively infrequent and difficult to detect. The kinetic coefficient for step advancement at different temperatures as well as the activation energy for incorporation of growth units into the surface (70.7 kJ mol^{-1}) is also well characterized. At very low supersaturation, the crystal growth kinetics has been measured for the $\{010\}$ face of gypsum in contact with water collected from the Naica mine at temperatures in the $50\text{--}90^\circ\text{C}$ range using an advanced high-resolution white-beam phase-shift interferometry microscope.³³ The growth rates found in this work for temperatures in the $50\text{--}55^\circ\text{C}$ range are extremely slow, ranging from 1.6×10^{-6} to $2.1 \times 10^{-5} \text{ nm s}^{-1}$. At this ultra-slow rate, to grow a giant crystal 1 m thick perpendicular to the $\{010\}$ face takes between 10^6 years and 10^5 years. Age estimates based on crystal growth kinetics assume that the growth is continuous and that there are no fluctuations in the growth rate at lower temperatures, which would locally increase the growth rate, nor at higher temperatures, which would slow down crystal growth and, eventually, stop growth or cause slow dissolution at the crystal surface. In fact, the best method for dating the age of a mineral process is the use of radiometric studies, such as uranium–thorium dating. Unfortunately, in the case of Naica gypsum crystals, particularly in the deeper caves of the mine, the concentration of uranium in the crystals is very low so that the uncertainty of the radiometric measurement is important. Nonetheless, it yields preliminary results that confirm that the crystal growth process of giant crystals started at least 400 Ky ago.^{17,37,40,41} Therefore, while it is expected that the use of new technologies will allow dating the age of different crystals in the Naica mountain and their growth history in the future, the experimental measurement of crystal growth kinetics is an interesting tool to analyse the current and further radiometric dating of crystals.

Screw dislocations and similar crystal defects that make the generation of new steps easier can be nucleated around impurities, for example colloidal particles, incorporated into the crystal surface, which is conceptually equivalent to heterogeneous nucleation, or around surface instabilities like macrosteps or fluid inclusions, which are quite frequent on the surface of gypsum crystals. Obviously, the giant gypsum crystals must grow by some of these mechanisms. Screw dislocations have seldom been observed on the $\{010\}$ face, although the observation of etch pits during dissolution experiments⁴² seems to suggest their presence. They are probably just difficult to observe due to the extremely anisotropic shape of two-dimensional nuclei and dislocation hillocks and the frequent presence of macrosteps. Whether the generation of steps during the growth of giant crystals is due to spiral growth or to other mechanisms is still an open question.

5.2 Crystal morphology

When entering the Cave of Crystals, it is surprising to find two completely different morphologies (Fig. 10), both of them already described by Foshag¹⁵ in the Cave of Swords. The walls and particularly the floor are sprinkled with blocky single crystals that in some cases cluster to form parallel or radial



Fig. 10 View of the Cave of Crystals in Naica showing the two clearly different morphologies present: blocky crystals (mostly to the right/bottom) and beams (left/top). Picture by Javier Trueba (msf).

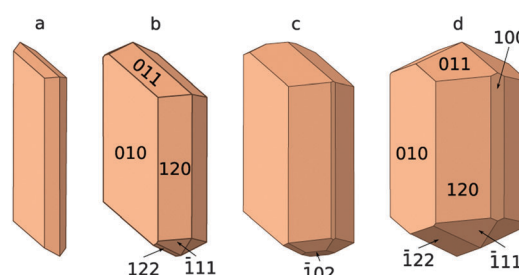


Fig. 11 Selection of published equilibrium morphologies for gypsum. (a) PBC morphology;⁴⁴ (b) refined PBC morphology;⁴⁵ (c) minimized surface energy morphology without surface relaxation and (d) with surface relaxation.⁷

aggregates while some much more elongated crystals grow from some of these groups of blocky crystals or directly from the floor, and some cross the cave from side to side.⁴³ These are the giant beams that make the Naica crystals so famous. To unveil such mystery we need some information on crystal morphology.

The equilibrium morphology of gypsum has been the subject of several papers, starting with the pioneering work by Simon and Bienfait⁴⁴ using PBCs and their later refinement by Weijnen *et al.*⁴⁵ These works, based on the “Periodic Bond Chain” (PBC) theory that defines the stability of surface features as a function of the directional distribution of bond energy, proposed faces $\{010\}$, $\{120\}$, $\{011\}$ and $\{\bar{1}11\}$, in decreasing order of morphological importance, as the four faces making up the equilibrium morphology of gypsum (Fig. 11a and b).

The crystals from Naica, grown very close to equilibrium, are an exceptional opportunity to study macroscopic equilibrium morphologies since crystals of more than one micron normally deviate from the equilibrium morphology because of their evolution during growth. Blocky crystals (Fig. 12) are single crystal prisms bounded by $\{010\}$ and $\{1k0\}$ faces and capped by $\{\bar{1}11\}$ faces.⁴³ The $\{1k0\}$ faces, whose existence in the



Fig. 12 Morphology of a typical blocky crystal from the Cave of Crystals showing the $\{010\}$, $\{1k0\}$ and $\{\bar{1}11\}$ main forms. The $\{011\}$ form is only marginally present in the incomplete, truncated uppermost corner.

equilibrium morphology of gypsum was discovered by studying the giant Naica crystals, are striated and composed of alternating bundles of $\{120\}$, $\{140\}$ and $\{160\}$ faces making an overall orientation close to $\{140\}$. This morphology deviates in some aspects from the equilibrium morphology known at that time: the more developed faces in the giant crystals are the $\{1k0\}$ family instead of $\{010\}$, the one predicted by theory; several faces in this family (at least $2 \leq k \leq 6$) appear and the overall face is $\{140\}$ instead of $\{120\}$. In addition, $\{\bar{1}11\}$ is more developed than $\{011\}$. Soon after the description of the morphology of the giant Naica crystals, these contradictions gave a boost to new investigations on the equilibrium morphology of gypsum, leading to explanations of these observations by refining the surface energy calculations taking into consideration surface relaxation and semi-empirical potentials carefully selected for each interaction.⁷ The new equilibrium morphology is shown in Fig. 11c (without relaxation) and d (with relaxation). The origin of the striated $\{1k0\}$ forms was also explained using similar methods in ref. 46.

The second type of morphology is the colossal beams. All the beams are twins, *i.e.* crystalline assemblages composed of two or more single crystals growing together and with orientations related by a subset of the crystal symmetry group. There are different types of twins reported for gypsum.^{47–49} The Naica beams are $\{100\}$ contact twins, formed by two single crystals growing side by side separated by a $\{100\}$ surface. Fig. 13 shows the two single crystals (blue and brown) growing side by side along the 100 plane (grey surface). This gypsum twin, along with the overall role of the $\{100\}$ plane in crystal growth, has been revisited recently in the light of the study of the Naica giant crystals, leading to a deeper understanding of the role of this surface, and others in the same zone, in the crystal growth and morphology of gypsum.⁵⁰

It is known that gypsum crystals grown in the lab at high supersaturation have a more elongated or even acicular habit, but this cannot be the explanation in the Cave of Crystals

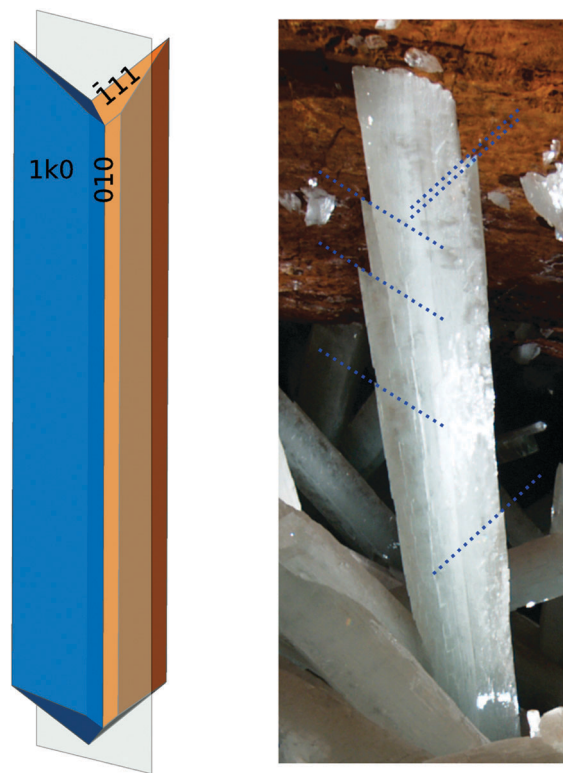


Fig. 13 Geometry of the $\{100\}$ contact twin in gypsum (left). The contact plane between both individuals is shown in transparent grey. Notice the re-entrant angle between $\{\bar{1}11\}$ faces on top. Twinned beam from the Cave of Crystals (left); the edges of $\{\bar{1}11\}$ faces are indicated by blue dotted lines.

because we know that the giant crystals grew from very low supersaturation solutions. Actually the colossal size of the beams is due to their twin character and the $\{100\}$ contact twin plays a subtle, yet fundamental, role in the development of the giant crystals, something that qualifies as the last ingredient needed to understand the beauty of these crystals. An important point about twins is that they can have reentrant dihedral angles (as shown in the upper part of Fig. 13), in contrast to single crystals that are, by definition, convex bodies. It is known that reentrant angles in crystals can work as a source of steps,⁵¹ and the generation of steps is the main factor limiting crystal growth rate at low supersaturation. More recent investigations on this effect⁵² have concluded that (a) it can operate only under low supersaturation in crystals containing no screw dislocations and is less effective with an increasing number of these defects; (b) twinned crystals often show elongated morphology due to the enhanced growth rate in the crystallographic direction of the reentrant angle; (c) twinned crystals grow much larger than the coexisting single crystals and (d) they sometimes show crystal faces uncommon for single crystals. All these features are exhibited by the twin beams in the Cave of Crystals, which makes them so different from the blocky crystals precisely because of these characteristics. The elongated giant crystals in Naica are, consequently, precisely those crystals that developed, by chance, $\{100\}$ contact twins with the reentrant angle between their $\{\bar{1}11\}$ faces pointing approximately upwards.

6 Concluding remarks

The formation of giant crystals of gypsum in the Naica range in Mexico is the result of a nucleation process taking place at very low supersaturation and slow growth driven by either continuous or episodic supply of calcium sulphate over hundreds or thousands of years. That combination of very unlikely geochemical conditions is the result of a self-feeding mechanism based on a solution-mediated anhydrite–gypsum phase transition occurring in a slow and smooth cooling scenario with small amplitude thermal fluctuations. The famous giant crystal-line beams of Naica are twinned crystals whose growth along the *c*-axis was made faster by a reentrant angle enhanced growth mechanism.

The ten years path taken from the initial awe at the beauty of these crystals to the current understanding of their formation has been worth the effort. The technology has been pushed both to measure the extremely slow growth rates using *ad hoc* confocal differential interference microscopy and white beam interferometry³³ and to develop a technology for gypsum to measure homogenization temperature from single phase fluid inclusions,²⁸ thus allowing the estimation of the growth temperature of any crystal from Naica, no matter its location. On the scientific side, we have also learned about crystal nucleation and growth at very low supersaturation²¹ and about the equilibrium morphology,⁷ for which these crystals are the only possible experimental counterparts since actual laboratory experiments are not feasible.

In the near future, the giant gypsum crystals will continue inspiring further research to answer the questions still open on their origin. More conclusive results on the growth temperature and the detailed growth history (including the possibility of episodic growth) are expected to arise from (a) new data on the current temperature distribution and the fluid dynamics in the Naica underground, as well as a geothermal model; (b) high precision methods to determine the age and growth temperature across different locations of the crystals and (c) new experimental data on the solubility, surface energy and the nucleation behaviour of gypsum. Furthermore, this unique natural experiment is also expected to inspire advances in basic crystallization science, in particular in the understanding of growth mechanisms at very low supersaturation, and the origin of twins and their influence on the growth of crystals and their morphology.

Acknowledgements

We acknowledge support from “Factoría de Cristalización” (Consolider Ingenio 2010, Spanish MINECO), the Junta de Andalucía (project RNM5384) and the Spanish MICINN (projects CGL2010-16882 and AYA2009-10655). We thank our colleagues in previous studies in particular Prof. Carlos Ayora, Dr Angels Canals, and Dr Alexander van Driessche for interesting discussions and Javier Trueba for pictures of the Naica crystals. Eng. Roberto Carlos Reyes and Eng. Roberto Villasuso are acknowledged for information and discussions on the

geology of Naica and Compañía Peñoles for the facilities provided during the field studies.

References

- 1 J. Verne, *Voyage au centre de la Terre*, Hetzel, Paris, 1864.
- 2 G. Sand, *Voyage dans le cristal*, Ombres, Toulouse, 1993.
- 3 D. Hernando, *Superman: La creación de un superhéroe*, Timunmas, 2013.
- 4 C. Palache, *Am. Mineral.*, 1932, **17**, 362–363.
- 5 P. C. Rickwood, *Am. Mineral.*, 1981, **66**, 885–907.
- 6 J. M. García-Ruiz, A. Canals and C. Ayora, *McGraw-Hill Yearbook Sci. Technol.*, 2008, 2008, pp. 154–156.
- 7 F. R. Massaro, M. Rubbo and D. Aquilano, *Cryst. Growth Des.*, 2010, **10**, 2870–2878.
- 8 C. Klein, *Manual Of Mineral Science*, John Wiley & Sons, 22nd edn, 2002.
- 9 J. Glater, J. L. York and K. S. Campbell, in *Principles of desalination*, ed. K. Spiegler, Academic Press, 2nd edn, 1980, ch. 10, pp. 627–678.
- 10 A. E. S. Van Driessche, L. G. Benning, J. D. Rodriguez-Blanco, M. Ossorio, P. Bots and J. M. García-Ruiz, *Science*, 2012, **336**, 69–72.
- 11 R. J. Erwood, S. E. Kesler and P. L. Cloke, *Econ. Geol. Bull. Soc. Econ. Geol.*, 1979, **74**, 95–108.
- 12 J. R. Lang, *A geological evaluation of the Naica deposit, Chihuahua, Mexico*, Internal Report of Compañía Fresnillo, Mexico Technical Report 109, 1995.
- 13 L. M. Alva-Valdivia, A. Goguitchaichvili and J. Urrutia-Fucugauchi, *Earth, Planets Space*, 2003, **55**, 19–31.
- 14 F. M. Haynes and S. E. Kesler, *Econ. Geol.*, 1988, **83**, 1985–1992.
- 15 W. Foshag, *Am. Mineral.*, 1927, **12**, 252–256.
- 16 N. Degoutin, *Soc. Cient. Antonio Alzate Rev.*, 1912, **32**, 35–38.
- 17 F. Gázquez, J. M. Calaforra, P. Forti, F. Rull and J. Martínez-Fras, *Int. J. Speleol.*, 2012, **41**, 211–220.
- 18 J. M. García-Ruiz, A. E. S. Van Driessche, J. M. Delgado, A. Canals and M. Ossorio, *Macla*, 2011, **15**, 13–14.
- 19 P. K. M. Megaw, J. Ruiz and S. R. Titley, *Econ. Geol. Bull. Soc. Econ. Geol.*, 1988, **83**, 1856–1885.
- 20 J. G. Stone, *Econ. Geol. Bull. Soc. Econ. Geol.*, 1959, **54**, 1002–1034.
- 21 J. M. García-Ruiz, R. Villasuso, C. Ayora, A. Canals and F. Otálora, *Geology*, 2007, **35**, 327–330.
- 22 D. Kashchiev, *Nucleation*, Butterworth-Heinemann, 1st edn, 2000.
- 23 K. F. Kelton and A. Greer, *Nucleation in Condensed Matter Applications in Materials and Biology*, Pergamon, vol. 15, 2010.
- 24 D. Gebauer and H. Cölfen, *Nano Today*, 2011, **6**, 564–584.
- 25 A. Lancia, D. Musmarra and M. Prisciandaro, *AIChE J.*, 1999, **45**, 1547–5905.
- 26 J. Merkel Broder and B. Planer-Friedrich, *Groundwater Geochemistry. A Practical Guide to Modeling of Natural and Contaminated Aquatic Systems*, Springer-Verlag, Berlin Heidelberg, 2nd edn, 2008.

- 27 D. L. Parkhurst and C. A. J. Appelo, *User's guide to PHREEQC (Ver. 2). A computer program for speciation, reaction-path, 1D-transport, and inverse geochemical calculations*, US Geol Surv Water Resour Invest Rep 99-4259, 1999.
- 28 Y. Krüger, J. M. García-Ruiz, A. Canals, D. Marti, M. Frenz and A. E. S. Van Driessche, *Geology*, 2013, **41**, 119–122.
- 29 C. W. Blount and F. W. Dickson, *Am. Mineral.*, 1973, **58**, 323–331.
- 30 E. P. Partridge and A. H. White, *J. Am. Chem. Soc.*, 1929, **51**, 360–370.
- 31 E. Posnjak, *Am. J. Sci.*, 1938, **235A**, 247–272.
- 32 L. A. Hardie, *Am. Mineral.*, 1967, **52**, 171–200.
- 33 A. E. S. Van Driessche, J. M. García-Ruiz, K. Tsukamoto, L. D. Patiño Lopez and H. Satoh, *Proc. Natl. Acad. Sci. U. S. A.*, 2011, **108**, 15721–15726.
- 34 F. Gázquez, *Quaternary International*, 2012, **279–280**, 162–163.
- 35 J. M. García-Ruiz, *J. Struct. Biol.*, 2003, **142**, 22–31.
- 36 J. W. Mullin, *Crystallization*, Butterworth Heinemann, 3rd edn, 1997.
- 37 L. Sanna, P. Forti and S. E. Lauritzen, *Acta Carsologica*, 2011, **40**, 17–28.
- 38 A. Van Driessche, F. Otálora, G. Sasaki, M. Sleutel, K. Tsukamoto and J. Gavira, *Cryst. Growth Des.*, 2008, **8**, 4316–4323.
- 39 A. E. S. Van Driessche, J. M. García-Ruiz, J. M. Delgado-López and G. Sasaki, *Cryst. Growth Des.*, 2010, **10**, 3909–3916.
- 40 L. Sanna, F. Saez, S. Simonsen, S. Constantin, J. M. Calaforra, P. Forti and S. E. Lauritzen, *Int. J. Speleol.*, 2010, **39**, 35–46.
- 41 S. E. Lauritzen, S. Constantin and P. Forti, *Chronology and growth rate of the Naica giant gypsum crystals*, International Geological Congress Oslo 2008, Oslo. <http://www.cprm.gov.br/33IGC/1322921.html>, 2008.
- 42 M. Peruffo, M. M. Mbogoro, M. A. Edwards and P. R. Unwin, *Phys. Chem. Chem. Phys.*, 2013, **15**, 1956–1965.
- 43 J. M. García-Ruiz, R. Villasuso, C. Ayora, A. Canals and F. Otálora, *The Formation of Natural Gypsum Megacrystals in Naica (Mexico)*, Data repository item DR2007080, 2007.
- 44 B. Simon and M. Bienfait, *Acta Crystallogr.*, 1965, **19**, 750–756.
- 45 M. P. C. Weijnen, G. M. van Rosmalen, P. Bennema and J. J. M. Rijkema, *J. Cryst. Growth*, 1987, **82**, 509–527.
- 46 F. R. Massaro, M. Rubbo and D. Aquilano, *Cryst. Growth Des.*, 2011, **11**, 1607–1614.
- 47 R. D. Cody and A. M. Cody, *J. Sediment. Res.*, 1988, **58**, 247–255.
- 48 M. Rubbo, M. Bruno, F. R. Massaro and D. Aquilano, *Cryst. Growth Des.*, 2012, **12**, 264–270.
- 49 M. Rubbo, M. Bruno, F. R. Massaro and D. Aquilano, *Cryst. Growth Des.*, 2012, **12**, 3018–3024.
- 50 M. Rubbo, M. Bruno and D. Aquilano, *Cryst. Growth Des.*, 2011, **11**, 2351–2357.
- 51 P. Hartman, *Z. Kristallogr.*, 1956, **107**, 225–237.
- 52 M. Kitamura, S. Hosoya and I. Sunagawa, *J. Cryst. Growth*, 1979, **47**, 93–99.